PORT SAID ENGINEERING RESEARCH JOURNAL
Faculty of Engineering - Port Said University
Volume 29 No. 3 pp: 18:37

Second Order Inelastic Analysis of Steel Space Frames Subjected to Span Loads

Abbad-Elrahman Farag [1], Tarek Sharaf[2], Mohamed Elghandour[3], Ashraf El-Sabbagh[4]*

[1] *Civil Engineering Department, Faculty of Engineering, Port Said University, Port Said, Egypt, email: abbad.farg@gmail.com*
[2] *Civil Engineering Department, Faculty of Engineering, Port Said University, Port Said, Egypt, email: tarek.sharf @eng.psu.edu.eg.com*
[3] *Civil Engineering Department, Faculty of Engineering, Port Said x University, Port Said, Egypt, email: drelghandor@gmail.com*
4 Civil Engineering Department, Faculty of Engineering, Port Said *University,* Port Said, Egypt, *email: ashref.ismail @eng.psu.edu.eg.com*
**Corresponding author,* *DOI: 10.21608/pserj.2025.373401.1402*

Received 7-4-2025,
Revised 23-4-2025,
Accepted 27-4-2025

ABSTRACT

This work provides a new model for the advanced analysis of steel frames subjected to span loads. The proposed model tries to overcome many issues of the analysis. A one element per member concept is used. Large deflection effects are considered by employing fifth order displacement function that takes member lateral loads into consideration. The interaction between the axial force effect and flexural actions is taken into consideration including the actions due to span loads. Plasticity spread along the member span is traced and modeled by monitoring number internal section along the span, then plasticity effects at these sections are merged in the one element stiffness matrix. This model helps to overcome limitations related to one element approach, as most one element models allow nodal loads only, or concentrated plasticity. The accurate representation of plasticity spread in the present model enables the model to take into consideration the variation in fixed end forces due to material yielding. A finite element program is prepared based on the proposed model. Many steel frames are solved and the results are compared with solutions by other research or by solutions from fine mesh analysis. The proposed model presented high accuracy without much calculation cost.

Keywords: Plasticity Spread, Three-dimensional Frames, Span Loaded Element, Second Order analysis, Beam-Column Element

1 INTRODUCTION

Many steel design specifications have considered the method of direct analysis which allows representing the second order effect by performing nonlinear analysis [1]. That's why the concept of advanced analysis of steel frames attracted more attention of structural engineering research studies [2], [3]. Structural engineers usually employ computer models based on finite element analysis for the purpose of steel frame analysis and design. During steel frames modelling, finite element models (FEM) based on solid or shell elements can represent the behavior of structures producing more accurate results than the FEM based on beam-column element. However, the mentioned accuracy of solid and shell FEM costs much time for modelling and calculations. That's why most steel structure engineers employ beam-column elements in their models. Consequently, the goal of many researchers was to improve the abilities of beam-column elements to accurately represent steel members nonlinear behavior accurately without costing much calculations.

To include large deflection effects in the beam-column element, Oran [4] employed stability functions in the analysis of planner and space frames, however, convergence issues appeared sometimes due to the different formulas for tension and compression. These stability functions were employed in many research studies with various additions to include different effects of geometric nonlinearity such as, torsional stiffness modifications [5], member initial imperfection [6], and lateral torsional buckling [7].

Research studies tried to work on polynomial shape functions with the principle of minimum potential energy to drive a beam-column element that can overcome the convergence issues of stability functions element. Based on a third order shape function, Meek

and Tan [8] generated the well-known cubic element and employed it in nonlinear analysis of space frames. Many publications included research studies on structural analysis of frames based on cubic element such as the work in [9]. Teh [10] investigated the accuracy and reliability of that element to represent steel space frames and concluded that frame member should be divided into more than one cubic beam column element in the analysis to obtain a sufficient accuracy.

At this point, the nonlinear analysis of framed structures faced two problems, the first was convergence issues when using stability functions and the second was the accuracy when using one cubic element per member. In 1994, based on a shape function of fifth order, Chan and Zhou [11] found the point wise equilibrium element (PEP) which achieved an obvious progression by Tackling mentioned issues of both stability functions and cubic element. They extended their work to include geometric imperfection to the element [12], and also many other researchers used the (PEP) element in their work either by employing it directly in their analysis or by making modifications on it [13],[14]. Also, the effect of shear deformation was included in the (PEP) element [15] to enhance its accuracy in different conditions of analysis. The advantages of stiffness coefficients produced by -PEP- element encouraged other researchers like Iu. and Bradford [16] to develop other beam-column elements based on polynomial fourth order shape function.

Practical advanced analysis requires representing both geometric and material nonlinear effects to achieve optimum design of steel frames [17]. Beam-column elements were utilized in the advanced analysis of frames by many methods of modelling both geometric and material nonlinearity. The different methods of inelastic analysis consider material yielding either as lumped plasticity at member nodes or distributed plasticity along the member. Plastic hinge analysis, which represents plasticity concentrated at nodes, requires less calculations and attracted the attention of research studies along the years [18], [19]. Chen and Chan [20] developed one beam column element with three nodes and three probable plastic hinges, two at member ends and one at mid span.

During plastic hinge analysis, zero length rotational springs are considered which encouraged research studies such as [21], [22], [23] to model frames employing plastic hinge concept and including effect of joints' semi-rigidity. Also, Refined plastic hinge method was developed [24], which allowed the gradual yielding of hinges to be captured and modeled presenting more accuracy, that made it more desirable by researchers and widely used in the analysis [25], [26], [27], [28]. Zhue *et al*.[29], [30] improved the refined plastic hinge to make it represent the local buckling and strain hardening of material effects. S. Lee *et al*. [31] used plastic hinge analysis to produce a large amount of data set, which was employed in training machine learning models that can help in predicting positions of probable plastic hinges for structures without performing the nonlinear analysis.

Unlike plastic hinges that are based on yielding surface equations, S. Kim *et al*. [32] used fiber hinge model that was based on dividing the cross section in many fibers. That fiber hinge has a length of the member can model plasticity at this length only, also a third one can be modeled along the span. The length of fiber hinge can affect the accuracy of the analysis [33], [34]. Nguyen and Kim[35] used fiber hinge to capture plasticity effects while working on modes that can calculate lateral torsional buckling. Although the fiber hinge coasts additional calculations during analysis, plasticity spread is neglected at member zones rather than the fiber hinge zones. Also, Zhou *et al*. [36] tried to capture span plasticity by allowing a refined plastic hinge to form at an arbitrary location along the span with the consideration of residual stresses effect. The distributed plasticity along the span can be traced with more accuracy using plastic zone analysis instead of plastic hinge. The early work by Elzanaty [37] aimed to produce accurate calculation of steel frames with distributed plasticity. Through years, researchers tried to develop techniques for plastic zone analysis with more simplicity in modelling and a smaller number of calculations with satisfying accuracy. Chiorean and Barasan[38] employed flexibility approach to find beam column elements that can trace distributed plasticity, and the work was extended for tapered members [39] and semi rigid frames [40]. Du. *et al*. [41] included geometric imperfection and shear deformation in their force-based analysis for distributed plasticity, while Chen *et al.* [42] included geometric imperfection on flexibility-based analysis for tarped elements. Displacement-based analysis was used by others, such as Viana *et al*. [43], Zubydan [44], for plastic zone analysis, however they had to use more than one element for each frame member to trace span yielding. Formulas can be used in tracing plasticity spread across the section of the element, such as the proposed in [44], [45], [46], [47], [48], which are available for different loading directions on I-shaped and H-shaped cross-sections. Zubydan *et al*. [49] developed their equivalent accumulated element to represent distributed plasticity, however their model is limited to elements under nodal forces only.

Unlike many beam-column analysis which assume loads to be nodal only, Zhou and Chan [50] modified the PEP element to allow member distributed loads for elastic analysis. Kim and Choi [51] used stability functions with refined plastic hinges for modelling frame elements with span loads. The derivation of second order stiffness coefficients can be affected by the types and shapes of loads, that can lead to different second order stiffness factors for each load shape. Trying to find an element with generalized load, Iu. and Bradford [52] developed their work on the fourth order shape function in [16] to produce element with

transverse loads. The concept of generalized element load used in [52] was employed by Iu. [53] reproducing the fifth order shape function for the element with transverse loads. To add material nonlinearity to the analysis of frames with span loads, the well-known refined plastic hinges analysis can be employed such as [54], however, the plasticity spread along the span can't be captured without dividing the member to many elements. Lateral span loads on frame element increase the probability of yielding along the member length. At the present work, the authors aim to develop a beam-column element that can represent the member with span loads using a single element per member during second order analysis but considering distributed plasticity. The research overcomes the obstacles of misleading results of concentrated plasticity assumption. Unlike many other research studies, the effect of plasticity spread on converting span loads into nodal forces is captured and represented accurately in the present work.

2 ELASTIC ELEMENT MODEL

This section demonstrates the stiffness relations for the element shown in Figure 1. These relations were firstly deduced in [50] to allow the element span loads to be included in the elastic second order analysis. They have derived a fifth order shape function, which has been rearranged in the present work in Eq. 1, considering the bending moment at mid-span due to lateral loads, M_0, as a part of the boundary conditions.

$$v = \mathrm{N}_1 L\theta_{z1} + \mathrm{N}_2 L\theta_{z2} - N_m L\overline{M_0} \tag{1.a}$$

$$\begin{aligned} N_1 = \Bigg[\xi &- \frac{0.5(5q+48)\xi^2}{q+48} + \frac{(4q)\xi^3}{q+48} \\ &- \frac{(2q)\xi^4}{q+48} \\ &- \frac{0.5(7q+240)\xi^2}{q+80} \\ &+ \frac{(80+9q)\xi^3}{q+80} - \frac{(10q)\xi^4}{q+80} \\ &+ \frac{(4q)\xi^5}{q+80}\Bigg] \end{aligned} \tag{1.b}$$

$$\begin{aligned} N_2 = \Bigg[\frac{0.5(5\mathrm{q}+48)\xi^2}{q+48} &- \frac{(4q)-\xi^3}{q+48} + \frac{(2q)\xi^4}{q+48} \\ &- \frac{0.5(7q+240)\xi^2}{q+80} \\ &+ \frac{(80+9q)\xi^3}{q+80} - \frac{(10q)\xi^4}{q+80} \\ &+ \frac{(4q)\xi^5}{q+80}\Bigg] \end{aligned} \tag{1.c}$$

$$N_m = \frac{16}{(q+48)}(\xi^2 - 2\xi^3 + \xi^4) \tag{1.d}$$

Where, $q = PL^2/EI_z$, $\xi = x/L$, and $\overline{M_0} = LM_0/EI$

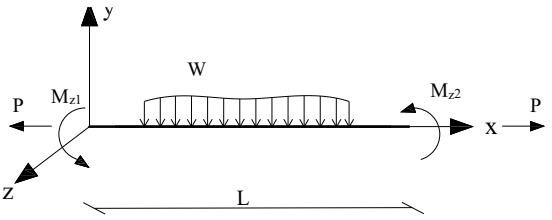

Figure 1: Member under equilibrium including span loads effects

Using the principle of total potential energy, the relations for secant stiffness can be found, as shown in Eq. 2 to Eq. 5. Where U is the strain energy, R is the work done by nodal forces, and T is the work done by span loads

$$\Omega = U - R - T \tag{2}$$

$$U = \frac{1}{2}\int_0^L EA\dot{u}\,dx + \frac{1}{2}\int_0^L EI\ddot{v}\,dx + \frac{1}{2}\int_0^L P\dot{v}\,dx \tag{3}$$

$$R = \sum_{i=1}^{3} F_i\gamma_i \tag{4}$$

$$T = \int_0^L w(x)v\,dx \tag{5}$$

Where, u is the axial shape function, w(x) is the element span load function, F_i *and* γ_i is the nodal are the nodal forces and their corresponding displacements. The equilibrium equation can be deduced from the first variation of the total energy function as $\partial\Omega = 0$. After performing the equilibrium, the secant relations can be found. It is worth mentioned that the differential operator in the expression $\partial\Omega$ refers to $\partial\Omega/\partial\gamma_i + \partial\Omega/\partial q \times \partial q/\partial\gamma_i$. However, this equilibrium condition contains the term of energy due to span load function, which means each shape of span load can produce different expression for the stiffness coefficients. The equations from Eq. 6 to Eq. 12 present the elastic secant relations.

$$M_{z1} = C_{z1}\theta_{z1} + C_{z3}\theta_{z2} + C_w\overline{M}_0 + M_{z1}^{EQV} \tag{6}$$

$$M_{z2} = C_{z3}\theta_{z1} + C_{z2}\theta_{z2} - C_w\overline{M}_0 + M_{z2}^{EQV} \tag{7}$$

$$\begin{aligned} P = EA\Bigg(&\frac{\Delta u}{L} + b_1(\theta_{z1}+\theta_{z2})^2 \\ &+ b_2(\theta_{z1}-\theta_{z2})^2 \\ &+ b_s(\theta_{z1}-\theta_{z2})\overline{M_0} + b_w\overline{M_0}^2\Bigg) \end{aligned} \tag{8}$$

$$\begin{aligned} C_{z1} &= C_{z2} \\ &= \frac{EI_z\left(19200 + 800\mathrm{q} + \frac{61}{7}\mathrm{q}^2 + \frac{23}{1260}\mathrm{q}^3\right)}{L(q+80)^2} \\ &+ \frac{EI_z\left(2304 + 288\mathrm{q} + \frac{29}{5}\mathrm{q}^2 + \frac{11}{420}\mathrm{q}^3\right)}{L(q+48)^2} \end{aligned} \tag{9}$$

$$C_{z3} = \frac{EI_z\left(19200 + 800\mathrm{q} + \frac{61}{7}\mathrm{q}^2 + \frac{23}{1260}\mathrm{q}^3\right)}{L(q+80)^2} - \frac{EI_z\left(2304 + 288\mathrm{q} + \frac{29}{5}\mathrm{q}^2 + \frac{11}{420}\mathrm{q}^3\right)}{L(q+48)^2} \quad (10)$$

$$b_1 = \frac{\left(\frac{23q^3}{2520} + \frac{46q^2}{21} + \frac{2080}{7}q + 12800\right)}{(q+80)^3} \quad (11)$$

$$b_2 = \frac{\left(\frac{11q^3}{840} + \frac{66q^2}{35} + \frac{672}{5}q + 4608\right)}{(q+48)^3} \quad (12)$$

Where, $\theta_{z1}\ and\ \theta_{z1}$ are the nodal rotations, Δu is the axial shortening, $q = PL^2/EI_z$, and $\overline{M_0} = M_0 L/EI_z$.

The coefficients M_{z1}^{EQV} and M_{z2}^{EQV} are the equivalent values for converting element span loads to be nodal loads, known as fixed end moment.

The factors C_w, b_s, and b_w are the second order and bowing terms due to span load, these are affected by the term T in the equilibrium equation which depends on the equation of span load $w(x)$ as shown in Eq. 5. Which means new different factors for each shape of loading. These expressions represent the interaction between axial force and flexural coefficients related to span loads.

The work in [50] deduced the equations of these factors considering the span loads to be modeled in three different shapes. The first shape as one concentrated load at the mid-span, the second shape as two concentrated loads, and the third shape as uniformly distributed along the span, shown in Figure 2. These expressions for second order relations, found in [50], are used in the present work for their corresponding loading shapes but for distributed plasticity analysis that is going to be deduced in Section 3.

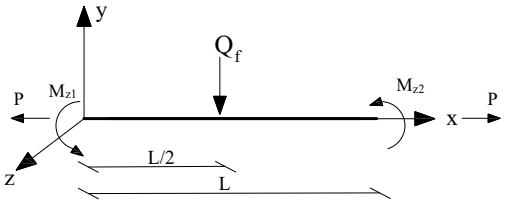

(a)

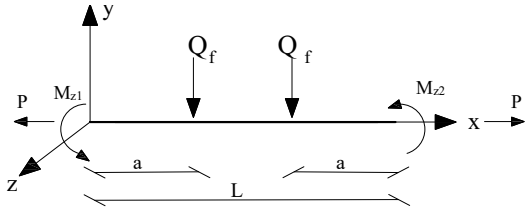

(b)

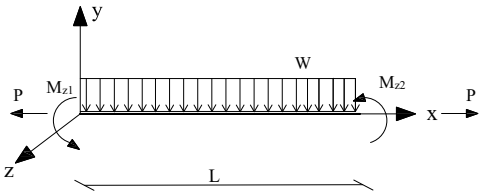

(c)

Figure 2: Member with Span Loads; a) One Concentrated Load , b) Two Concentrated Loads, c) Uniform Distributed Along The Span

For the element with distributed load on a part of the span, in Figure 3, the present work used the same methodology to provide new formulas for the coefficients C_w, b_s, and b_w in Eq. 13, Eq. 14, and Eq. 15, respectively. It can be noticed that, when the value of the distance a equals zero, the deduced expressions turn to be the same as the coefficients for the member shown in Figure 2.c. Another load shape is presented in Figure 4, which contains a member with triangular load. The same methodology was applied and the coefficients were deduced and presented in Eq. 17 to Eq. 20. Then, in the next step of the present work, all secant relations are going to be modified, in Section 3, to be capable of modelling inelastic behavior of the steel element, which is the major novel contribution of this work.

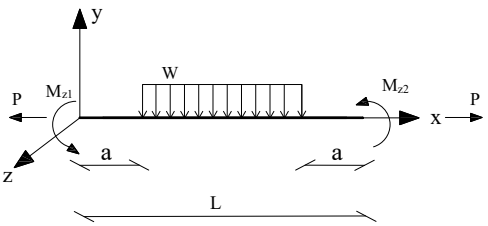

Figure 3: Member with Uniform Load on Part of Span

$$C_w = \frac{q(L-2a)^2(48aL+8L^2-48a^2)}{(q+48)(15L+30a)L^3} - \frac{q^2}{105(q+48)^2} \quad (13)$$

$$b_s = \frac{(L-2a)^2(768aL+128L^2-768a^2)}{(5L+10a)(q+48)^2L^3} - \frac{256q}{35(q+48)^3} \quad (14)$$

$$b_m = \frac{(L-2a)^2(384aL+64L^2-384a^2)}{(15L+30a)(q+48)^2L^3} - \frac{256(q+36)}{105(q+48)^3} \quad (15)$$

$$\overline{M_0} = \frac{L}{EI}\left(\frac{WL^2}{8} - \frac{Wa^2}{2}\right) \quad (16)$$

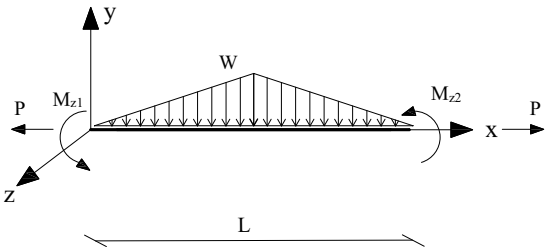

Figure 4: Member with Triangular Load

$$C_w = \frac{q(199q+11088)}{420(q+48)^2} \quad (17)$$

$$b_s = \frac{4(167q+11088)}{35(q+48)^3} \quad (18)$$

$$b_m = \frac{2(103q+6480)}{105(q+48)^3} \quad (19)$$

$$\overline{M_0} = \frac{WL^3}{12\,EI} \quad (20)$$

All the previously mentioned stiffness relations are available for elastic analysis only. However, the factors related to span loads can be specified as first and second order factors. The second order factors C_w, b_s, and b_w vanish when the axial force equals zero.

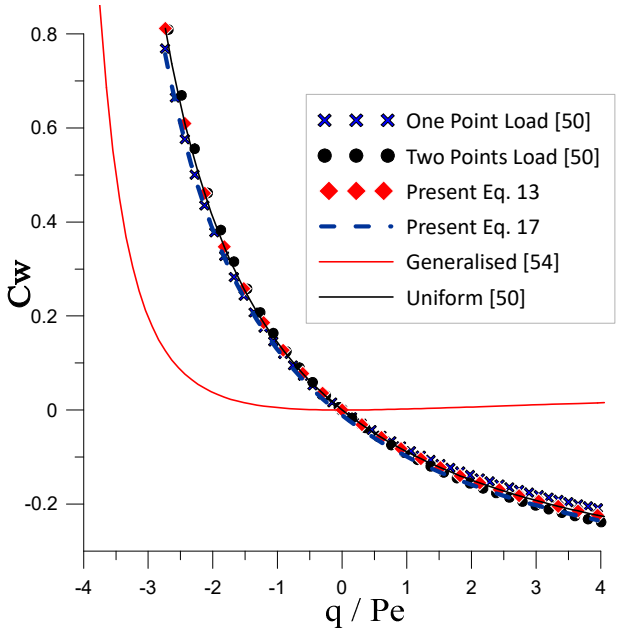

Figure 5: Comparison of Different Formulas to Calculate Second Order Coefficient C_w

The comparison shown in Figure 5 declares that the generalized formula deduced in [54] has a noticed difference from the calculated either by [50] or in the present work. That difference occurred as the work in [54] neglected the differentiation of the external work by span load, in Eq. 5, respect to the load parameter q. They assumed $\partial T/\partial q$ to equal zero, which affected the accuracy of their expressions. Although the main purpose of the present research is to develop inelastic relations for different load shapes as presented in Section 3, we did use the general expression by [54] due to its lack of accuracy. So, we have deduced our own accurate second order factors C_w, b_s, and b_w for each load shape solved this paper.

The first order factors M_{z1}^{EQV} and M_{z2}^{EQV} are not affected by the value of axial force, and they are deduced based on the linear displacement function as they can be deduced using Eq. 21 and Eq. 22.

$$M_{z1}^{EQV} = \int_0^1 \frac{\partial v_L}{\partial \theta_{z1}} w(x)dx \quad (21)$$

$$M_{z2}^{EQV} = \int_0^1 \frac{\partial v_L}{\partial \theta_{z2}} w(x)dx \quad (22)$$

Where, v_L is the linear shape function of the element, and $w(x)$ represents the equation of the load. For example, performing the integration in Eq. 21 and Eq. 22 for a uniformly distributed load with a value equals W produces values as $WL^2/12$ and $-WL^2/12$ for M_{z1}^{EQV} and M_{z2}^{EQV}, respectively.

3 INELASTIC ELEMENT MODEL

This section is dedicated to deriving the stiffness coefficients for the beam column element including span load effects. Firstly, the assumptions and main methodology of element formulations are presented. Then, the first order relations are deduced, which include stiffness coefficients and the converting span loads to nodal forces (fixed end moment). Finally, the first order coefficients, including plasticity spread effects, are replaced in the elastic second order coefficients to upgrade them for plastic analysis.

3.1 Assumptions

- Conservative span lateral loads are allowed.
- Plasticity is allowed to be distributed along the element span.
- Sections always are plane even after deformation
- Local buckling and lateral torsional buckling are not allowed.
- Shear deformation and warping effects are neglected, and members have bisymmetrical cross sections.
- Strain hardening of steel material is neglected.
- Large rotations and displacements with small strains are considered.

3.2 The Equivalent Accumulated Element

Steel frame members have constant section rigidity during elastic stage of the analysis process. However, when the values of stresses increase beyond yield limit the sectional rigidity decreases. Unlike the plastic hinge analysis assumption, the current work depends on assuming the plasticity to be allowed along the span,

which is more realistic and accurate of representing the frame element. In the present research, Section 4 provides a brief about how the plasticity spread is captured and the member with yielded parts is converted to the equivalent element and how the tangent rigidity of the sections is calculated.

As shown in Figure 6, the frame element with yielded parts is represented by one beam-column element with many internal segments each of them is allowed to have different values of EI. This variation of rigidity along the span affects not only the stiffness coefficients of the element, but also the values of fixed end moments transforming span loads to nodal forces. It must be notified that the values calculated from Eq. 21 and Eq. 22 are no longer accurate as they are first order forces based on linear shape function which is not applicable any more after plasticity existing.

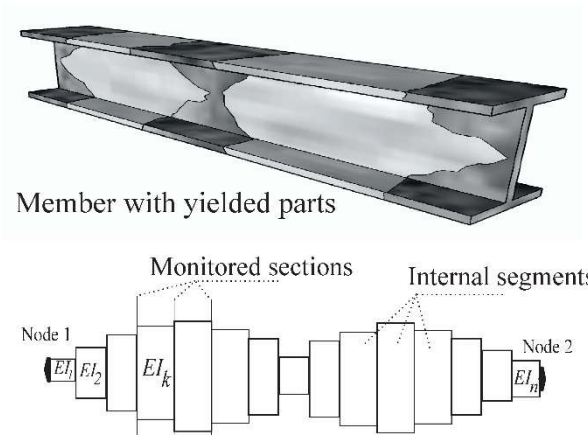

Figure 6: Tow Nodes Element Representing Member with Yielded Parts

3.3 First Order Relations for Degraded Element

This section is dedicated to deduce the expressions of first order relations considering the member to have span loads. The calculated relations include the first order stiffness coefficients and the first order fixed end moments, and both of them consider the member to have different values of *EI* for its internal segments as declared in Section 3.2.

For different span load shapes, the stiffness coefficients are the same while the fixed end moment relations change according to the shape of the load. The present work provided the solutions for five different shapes of loads which have been presented in Figure 2, Figure 3, and Figure 4.

3.3.1 Member with Uniform Distributed Load

The member is assumed to have many internal segments and each of them has a value of EI_z, which represents the inelastic section rigidity due to plasticity spread. As the plasticity has been already modelled by considering the different values of *EI* for the internal segments, so the member on its new conditions can be treated as elastic member, and the principles of Castigliano's second theorem can be applied. This theorem assumes the strain energy to be expressed as functions of the generalized forces, then performing a differentiation with respect to a generalized forces produces the corresponding displacement to it. So, strain energy can be expressed as shown in Eq. 23, and this equation can be differentiated with respect to M_{z1} and M_{z2} to get the expressions for θ_{z1} and θ_{z2}, respectively, shown in Eq. 24 and Eq. 25.

$$U = \int_0^1 \frac{M_z^2}{2EI_z} L d\xi \quad \text{where, } \xi = x/L \tag{23}$$

$$\theta_{z1} = \frac{\partial U}{\partial M_{z1}} = \int_0^1 \frac{M_z}{EI_z} \frac{\partial M_z}{\partial M_{z1}} L d\xi \tag{24}$$

$$\theta_{z2} = \frac{\partial U}{\partial M_{z2}} = \int_0^1 \frac{M_z}{EI_z} \frac{\partial M_z}{\partial M_{z2}} L d\xi \tag{25}$$

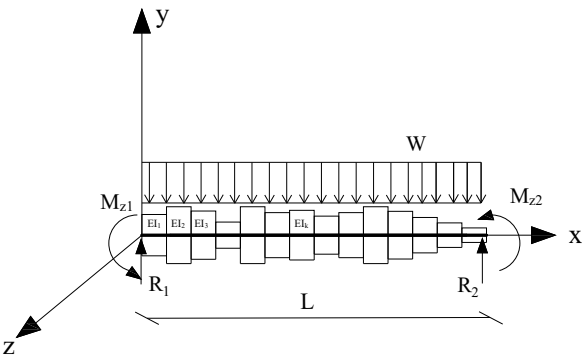

Figure 7: The Equivalent Element under Uniformly Distributed Span Load

For the member shown in Figure 7, we can simply find the equation on bending moment as presented in Eq. 26.

$$M_z = \left(M_{z1}(1-\xi) - M_{z2}\,\xi + \frac{WL^2}{2}(\xi^2 - \xi) \right) \tag{26}$$

By substituting in Eq. 24 and Eq. 25, the expressions of nodal rotations convert to be as following.

$$\theta_{z1} = \int_0^1 \frac{1}{EI_z} \left(M_{z1}(1-\xi) - M_{z2}\,\xi + \frac{WL^2}{2}(\xi^2 - \xi) \right) (1-\xi) L d\xi \tag{27}$$

$$\theta_{z2} = \int_0^1 \frac{1}{EI_z} \left(M_{z1}(1-\xi) - M_{z2}\,\xi + \frac{WL^2}{2}(\xi^2 - \xi) \right) (-\xi) L d\xi \tag{28}$$

The value of EI_z changes along the element span according to each internal segment, that's why we are

going to perform the integrations along an arbitrary segment K and accumulate the number n of internal segments along the element span. That makes the expressions of the nodal rotations to be as following.

$$\theta_{z1} = \sum_{k=1}^{n} \int_{\xi_{k-1}}^{\xi_k} \frac{1}{EI_z} \left(M_{z1}(1-\xi) - M_{z2}\,\xi + \frac{WL^2}{2}(\xi^2 - \xi) \right) (1-\xi) L d\xi \tag{29}$$

$$\theta_{z2} = \sum_{k=1}^{n} \int_{\xi_{k-1}}^{\xi_k} \frac{1}{EI_z} \left(M_{z1}(1-\xi) - M_{z2}\,\xi + \frac{WL^2}{2}(\xi^2 - \xi) \right) (-\xi) L d\xi \tag{30}$$

Now, we can perform multiplications and integrations in limits of the arbitrary segment. Also, the resulting equations can be arranged according to the terms of M_{z1}, M_{z2}, and W, and that generate the expressions from Eq. 31 to Eq. 37.

$$\theta_{z1} = M_{z1} S_{mz1} + M_{z2} S_{mz3} + S_{wz1} \tag{31}$$

$$\theta_{z2} = M_{z1} S_{mz3} + M_{z2} S_{mz2} + S_{wz2} \tag{32}$$

Where,

$$S_{wz1} = \frac{WL^3}{2} \sum_{k=1}^{n} \frac{1}{EI_{zk}} \left(-\frac{1}{4}\Delta\xi_k^4 + \frac{2}{3}\Delta\xi_k^3 - \frac{1}{2}\Delta\xi_k^2 \right) \tag{33}$$

$$S_{wz2} = \frac{WL^3}{2} \sum_{k=1}^{n} \frac{1}{EI_{zk}} \left(-\frac{1}{4}\Delta\xi_k^4 + \frac{1}{3}\Delta\xi_k^3 \right) \tag{34}$$

$$S_{mz1} = L \sum_{k=1}^{n} \frac{1}{EI_{zk}} \left(\Delta\xi_k - \Delta\xi_k^2 + \frac{1}{3}\Delta\xi_k^3 \right) \tag{35}$$

$$S_{mz2} = L \sum_{k=1}^{n} \frac{1}{EI_{zk}} \left(\frac{1}{3}\Delta\xi_k^3 \right) \tag{36}$$

$$S_{mz3} = L \sum_{k=1}^{n} \frac{1}{EI_{zk}} \left(-\frac{1}{2}\Delta\xi_k^2 + \frac{1}{3}\Delta\xi_k^3 \right) \tag{37}$$

Where, $\Delta\xi_k^i = \xi_k^i - \xi_{k-1}^i$, $\xi_k = x_k/L$, and K ranges from 1 to n number of segments.

To find the secant relations, we can solve Eq. 31 and Eq. 32 together and arranging the equations to be as following.

$$M_{z1} = C_{mz1}\,\theta_{z1} + C_{mz3}\,\theta_{z2} + MF_{z1} \tag{38}$$

$$M_{z2} = C_{mz3}\,\theta_{z1} + C_{mz2}\,\theta_{z2} + MF_{z2} \tag{39}$$

Where, C_{mz1}, C_{mz2}, and C_{mz3} are the first order secant stiffness coefficients. While C_{wz1} and C_{wz2} are the first order fixed end moments. The expressions from Eq. 40 to Eq. 44 show these coefficients after the final arrangement.

$$C_{mz1} = \frac{-S_{mz2}}{S_{mz3}^2 - S_{mz1}S_{mz2}} \tag{40}$$

$$C_{mz2} = \frac{-S_{mz1}}{S_{mz3}^2 - S_{mz1}S_{mz2}} \tag{41}$$

$$C_{mz3} = \frac{S_{mz3}}{S_{mz3}^2 - S_{mz1}S_{mz2}} \tag{42}$$

$$MF_{z1} = -S_{wz1}C_{mz1} - S_{wz2}C_{mz3} \tag{43}$$

$$MF_{z2} = -S_{wz2}C_{mz2} - S_{wz1}C_{mz3} \tag{44}$$

The deduced coefficients MF_{z1} and MF_{z2} vanish when there is no span lateral load applied. However, when there is a span load, these coefficients represent the first order fixed end moment considering the variation of the sections rigidity due to plasticity spread. During the earlier stages of an advanced analysis process, the member stills elastic and all the internal segments have the same value of EI_z. In this case, the deduced formulas for the coefficients of equivalent nodal forces C_{wz1} *and* C_{wz2} will finally convert to the results of $WL^2/12$ and $-WL^2/12$, the same as elastic conventional fixed end moments.

The same sequence can be adopted for different load shapes. The difference will be in the expression of bending moment which will affect only the coefficients S_{wz1}, *and* S_{wz2} and consequently MF_{z1} and MF_{z2}. And that makes sense as the stiffness coefficients are not affected by the span loads.

3.3.2 Member with Concentrated Load at Arbitrary Location

Considering the element shown in Figure 8, the same methodology in Section 3.3.1 can be applied using the appropriate expression of bending moment which should be presented in two parts as following in Eq. 45. Where $\xi = x/L$.

$$M_z = M_{z1}(1-\xi) - M_{z2}\,\xi - Q_f L(1-\xi_a)\xi \quad \text{For } \xi = 0 \text{ to } \xi_a \tag{45.a}$$

$$M_z = M_{z1}(1-\xi) - M_{z2}\,\xi + Q_f L\xi_a(\xi - 1) \quad \text{For } \xi = \xi_a \text{ to } 1 \tag{45.b}$$

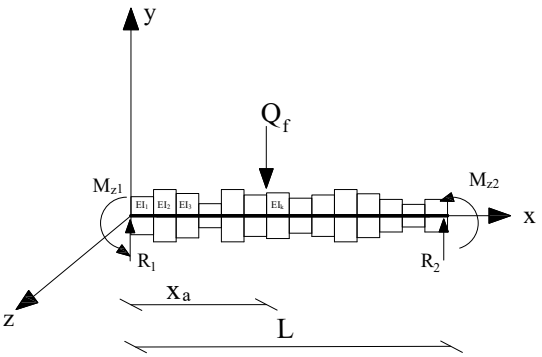

Figure 8: The Equivalent Element under One Concentrated Load at an arbitrary Location

The expression of moment changes depending on the value of ξ comparing to the value of ξ_a, so that, the integration along the span is going to be performed in parts each part uses its corresponding equation of moment as shown in Eq. 46 and Eq. 47.

$$\theta_{z1} = \int_0^{\xi_a} \frac{M_z}{EI_z}\frac{\partial M_z}{\partial M_{z1}} Ld\xi + \int_{\xi_a}^{1} \frac{M_z}{EI_z}\frac{\partial M_z}{\partial M_{z1}} Ld\xi \qquad (46)$$

$$\theta_{z2} = \int_0^{\xi_a} \frac{M_z}{EI_z}\frac{\partial M_z}{\partial M_{z2}} Ld\xi + \int_{\xi_a}^{1} \frac{M_z}{EI_z}\frac{\partial M_z}{\partial M_{z2}} Ld\xi \qquad (47)$$

After performing the integrations and arranging the formulas, all expressions in equations from Eq. 31 to Eq. 44 will be the same except the expressions for $S_{wz1}, and\ S_{wz2}$ that will change to be as shown in Eq. 48 and Eq. 49.

$$S_{wz1} = Q_f L^2 \left(\left(\sum_{k=1}^{a} \frac{(1-\xi_a)}{EI_{zk}} \left(\frac{1}{3}\Delta\xi_k^3 - \frac{1}{2}\Delta\xi_k^2 \right) + \sum_{k=a+1}^{n} \frac{\xi_a}{EI_{zk}} \left(-\frac{1}{3}\Delta\xi_k^3 + \Delta\xi_k^2 - \Delta\xi_k \right) \right) \right) \qquad (48)$$

$$S_{wz2} = Q_f L^2 \left(\sum_{k=1}^{a} \frac{(1-\xi_a)}{EI_{zk}} \left(\frac{1}{3}\Delta\xi_k^3 \right) + \sum_{k=a+1}^{n} \frac{\xi_a}{EI_{zk}} \left(-\frac{1}{3}\Delta\xi_k^3 + \frac{1}{2}\Delta\xi_k^2 \right) \right) \qquad (49)$$

For the load shape presented in Figure 2.a, in which the concentrated load locates at mid span, the formulas in Eq. 48 and Eq. 49 can be employed effectively by considering the value of ξ_a equals 0.5.

3.3.3 Member with Two Concentrated Loads at Symmetric Distance from Center

For the load shape shown in Figure 2.b, the element is subjected to two concentrated forces at symmetrical distance from both member ends. To be able to find the corresponding fixed end relations, we can apply the principles of super position. Instead of deducing fixed end moment for two loads, the present work has already found the formulas for fixed end moment due to one concentrated load located at an arbitrary location along the span, in Section 3.3.2. Regarding the first order relations, the concept of super position can be applied without compromising the results. The second order relations effects were found previously in [50]. For the case of two loads, the fixed end moment can be calculated separately for each of them and summation can be performed.

3.3.4 Member with Uniform Load on a Part of Span

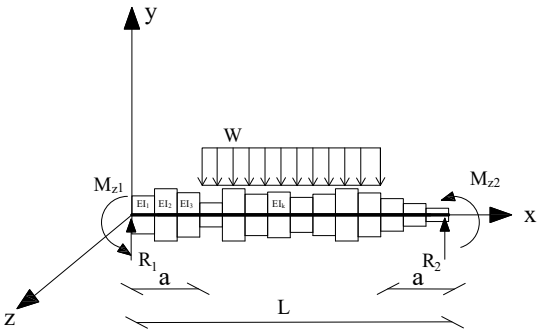

Figure 9: The Equivalent Element under Uniform Load Along Part of The Span

$$S_{wz1} = \frac{WL^3}{24}\left(\sum_{k=1}^{a}\frac{1}{EI_{zk}}\left(-8\xi_{\mathrm{a}}+4\right)\left(\Delta\xi_k^3-\frac{3}{2}\Delta\xi_k^2\right)\right.$$
$$+\sum_{k=a+1}^{(L-a)}\frac{1}{EI_{zk}}\left(-3\Delta\xi_k^4+8\Delta\xi_k^3+\left(-6{\xi_{\mathrm{a}}}^2-6\right)\Delta\xi_k^2+12{\xi_{\mathrm{a}}}^2\Delta\xi_k\right) \quad (50)$$
$$\left.+\sum_{k=(L-a)+1}^{n}\frac{1}{EI_{zk}}\left(8\xi_{\mathrm{a}}-4\right)\left(\Delta\xi_k^3-3\Delta\xi_k^2+3\Delta\xi_k\right)\right)$$

$$S_{wz2} = WL^3\left(\sum_{k=1}^{a}\frac{1}{EI_{zk}}\left(\frac{-\xi_{\mathrm{a}}}{3}+\frac{1}{6}\right)\left(\Delta\xi_k^3\right)+\sum_{k=a+1}^{(L-a)}\frac{1}{EI_{zk}}\left(\frac{-1}{8}\Delta\xi_k^4+\frac{1}{6}\Delta\xi_k^3-\frac{{\xi_{\mathrm{a}}}^2}{4}\Delta\xi_k^2\right)\right.$$
$$\left.+\sum_{k=(L-a)+1}^{n}\frac{1}{EI_{zk}}\left(\frac{\xi_{\mathrm{a}}}{3}-\frac{1}{6}\right)\left(\Delta\xi_k^3-\frac{3}{2}\Delta\xi_k^2\right)\right) \quad (51)$$

$$S_{wz1} = \frac{WL^3}{12}$$
$$\left(\left(\sum_{k=1}^{K=mid}\frac{1}{EI_{zk}}\left(-\frac{4}{5}\Delta\xi_k^5+\Delta\xi_k^4+\Delta\xi_k^3-\frac{3}{2}\Delta\xi_k^2\right)+\sum_{k=mid+1}^{n}\frac{1}{EI_{zk}}\left(\frac{4}{5}\Delta\xi_k^5-4\Delta\xi_k^4+7\Delta\xi_k^3-5\Delta\xi_k^2+\Delta\xi_k\right)\right)\right) \quad (53)$$

$$S_{wz2} = \frac{WL^3}{12}\left(\left(\sum_{k=1}^{K=mid}\frac{1}{EI_{zk}}\left(-\frac{4}{5}\Delta\xi_k^5+\Delta\xi_k^3\right)+\sum_{k=mid+1}^{n}\frac{1}{EI_{zk}}\left(\frac{4}{5}\Delta\xi_k^5-3\Delta\xi_k^4+3\Delta\xi_k^3-\frac{1}{2}\Delta\xi_k^2\right)\right)\right) \quad (54)$$

Using the same sequence first order relations for the load shape in Figure 9 can be found. However, in the present case, the integration process has to be performed in three intervals according to the variation in the expression of bending moment. The factors $S_{wz1}, and\ S_{wz2}$ are shown in Eq. 53 and Eq. 54.

Where, $\Delta\xi_k^i = \xi_k^i - \xi_{k-1}^i$ and the factor ξ_a depend on the shape of lateral load as $\xi_a = x_a/L$. It can be noticed that if $\xi_a = 0$, the expressions in Eq. 50 and Eq. 51 reach to be the same as in Eq. 33 and Eq. 34.

3.3.5 Member with Triangular Load

For the load shape in Figure 10, the expressions for first order secant relations can be found with the same previous procedure. It must be noticed during the derivation that the expression of bending moment is divided into two intervals as shown in Eq. 52. After performing the integrations, the coefficients of $S_{wz1}, and\ S_{wz2}$ corresponding to the triangular load can be derived as presented in Eq. 53 and Eq. 54.

$$M_z = M_{z1}(1-\xi) - M_{z2}\,\xi + \frac{WL^2}{12}(-3\xi + 4\xi^3) \quad (52.a)$$
For $\xi = 0\ to\ 0.5$

$$M_z = M_{z1}(1-\xi) - M_{z2}\,\xi + \frac{WL^2}{12}(1 - 9\xi + 12\xi^2 - 4\xi^3) \quad (52.b)$$
For $\xi = 0.5\ to\ 1$

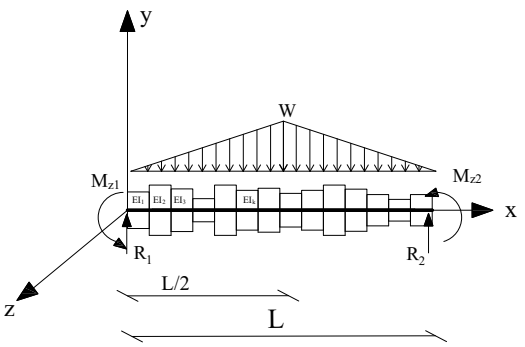

Figure 10: The Equivalent Element under Triangular Load

3.4 Inelastic Second-Order Secant and Tangent Relations

In the present work, the elastic second order relations have been presented in Section 2, while in Section 3.3 the inelastic first order relations have been presented. To

provide expressions that can include inelastic second order stiffness and fixed end moment, a technique of extraction and replacing is going to be considered. This technique was used previously in [49]. To get inelastic second order relations, two steps are going to be performed. The first is finding elastic second order relations, as provided in Section 2, these relations can be separated into first order and second order terms. The second step is finding the inelastic first order relations for the degraded member, as provided in Section 3.2, and replacing them instead of the previously separated elastic first order terms.

So, the bending coefficients in Eq. 9 and Eq. 10 can be modified by subtracting the elastic first order stiffness terms $4EI_z/L$ and $2EI_z/L$ and replacing them by the inelastic first order coefficients C_{mz1}, C_{mz2}, and C_{mz3} in Eq. 40 to Eq. 42. The same for the elastic conventional fixed end moment which is going to be replaced with the fixed end moment for degraded member in Eq. 42 and Eq. 43, deduced in Section 3.3, corresponding to the load shape. So, the secant relations reach the forms in Eq. 55 and Eq. 56

$$M_{z1} = \left(C_{mz1} + C_{gz1}\right)\theta_{z1} + \left(C_{mz3} + C_{gz2}\right)\theta_{z2} + C_w\bar{M}_0 + MF_{z1} \quad (55)$$

$$M_{z2} = \left(C_{mz2} + C_{gz1}\right)\theta_{z1} + \left(C_{mz3} + C_{gz2}\right)\theta_{z2} - C_w\bar{M}_0 + MF_{z2} \quad (56)$$

Where, the coefficients C_{mz1}, C_{mz2}, and C_{mz3} are calculated using the formulas from Eq. 40 to Eq. 42. While the factors MF_{z1}, and MF_{z2} are calculated using the formulas in Eq. 43 and Eq. 44 with the appropriate S_{wz1} and S_{wz2} depending on the load shape. The calculation of the second order term $C_w\bar{M}_0$ is detailed in Section 2. The factors C_{gz1} and C_{gz2} are shown in Eq. 57 and Eq. 58. The terms related to second order effects employ an equivalent value for EI_z of the degraded member as EI_{eqz} which has been discussed in detail in [49]. The used value for EI_{eqz} is considered to be the elastic rigidity in the present research.

$$C_{gz1} = \frac{EI_{eqz}}{L}\left(\frac{\left(\frac{23q^3}{1260} + \frac{40q^2}{7} + 320q\right)}{(q+80)^2} + \frac{\left(\frac{11q^3}{420} + \frac{24q^2}{5} + 192q\right)}{(q+48)^2}\right) \quad (57)$$

$$C_{gz2} = \frac{EI_{eqz}}{L}\left(\frac{\left(\frac{23q^3}{1260} + \frac{40q^2}{7} + 320q\right)}{(q+80)^2} - \frac{\left(\frac{11q^3}{420} + \frac{24q^2}{5} + 192q\right)}{(q+48)^2}\right) \quad (58)$$

Regarding the formulation of tangent stiffness matrix, Structure tangent stiffness matrix can be assembled as $K_T = \sum_{elements} L(T^T K_T^4 T)L^T$, where matrices [T] and [L] are to form the [12×12] matrix and to rotate the element from local to global coordinates, respectively. The matrix K_T and matrix T are presented in the appendix. The matrix L for rotating the element can be found in [26].

4 ANALYSIS PROCEDURE

4.1 Modelling Distributed plasticity

The present work aims to model steel frame members using one beam-column element for each member. Usually, researchers use concentrated plasticity approach for one element per member analysis. The current research assumes plasticity to be distributed along the member and trace this plasticity along the analysis process. Multiple cross sections along the span are going to be monitored along the analysis process. After calculating nodal displacements and forces for each load iteration, the applied forces on each monitored section are calculated using the member nodal forces, shape function, and span loads. The calculated actions on each monitored section are employed to evaluate the state of the cross section whether there is any yielding found or not.

The evaluation of yielding across the area of cross sections has been investigated by many researchers and various techniques were presented. The research studies in [44], [45], [47], [48] suggested formulas to calculate the tangent rigidity of the cross section without dividing the cross sections to many fibers. Formulas are available for different cross sections under different loading conditions including or neglecting residual stresses. The present research employs these formulas for the evaluation of cross sections during the analysis process, which means the whole analysis procedure is based on closed form solution and direct substitutions in previously deduced equations without additional numerical integrations.

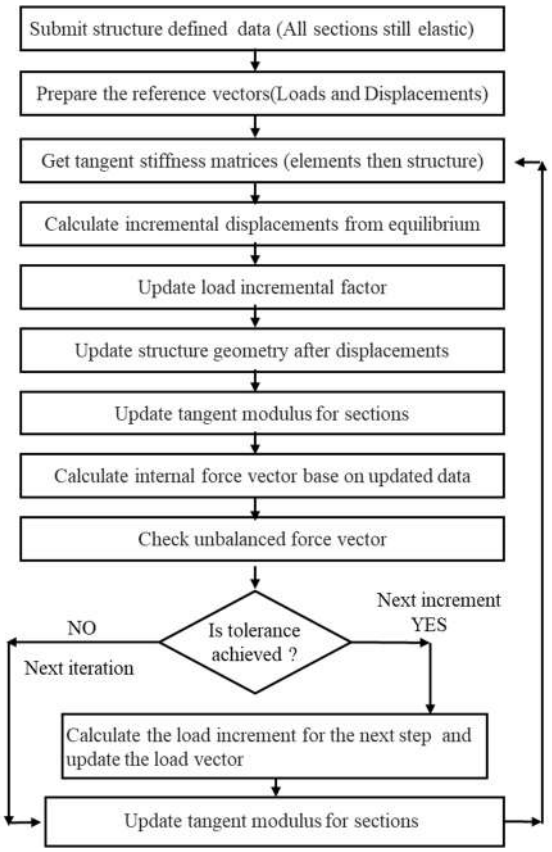

Figure 11: Analysis Flow Chart

At this point the beam-column element has multiple monitored sections and each of them has its own tangent rigidity during the inelastic stage of the analysis. That can transform the element to be consist of multiple internal segments with different values of $EI_{Tangent}$, and each internal segment starts and end with a monitored section. The internal segment's tangent rigidity is considered to be the average value of the values at the start and end monitored sections. The derivations in Section 3 were prepared based on the beam column element with multiple internal segments each of them has its own rigidity. That can trace plasticity spread along the member accurately.

4.2 Analysis Scheme

A finite element software was prepared to solve steel frames based on the numerical model of the present paper. Figure 11 illustrates the analysis procedure used in this program. It must be declared that, converting span loads to the equivalent nodal forces is already performed in the appropriate step of the analysis, either while updating the external load vectors or while calculating internal force vectors for equilibrium check. Each time these fixed end forces calculated; they are based on the last updated values of EI. This ongoing updating of the values of EI helps to maintain the accuracy of tracing plasticity spread and also to achieve rapid convergence of the analysis.

Throughout the analysis procedure, the incremental equilibrium equation will be as declared in Eq. 59 to start iteration number i at step number j.

$$[K_{i-1}^{j}]\{\Delta u_i^j\} = \{F_{ext\ i}^{j}\} - \{F_{int\ i-1}^{j}\} \quad (59)$$

where, $[K_{i-1}^{j}]$ is the last updated tangent stiffness matrix from iteration number i-1. And $\{\Delta u_i^j\}$ is the generated unbalanced displacement vector after solving the equilibrium condition. The vector $\{\Delta F_{i-1}^{j}\}$ is the last updated internal force vector from previous iteration. The vector $\{F_{ext\ i}^{j}\}$ is the external force vector, including fixed end forces, which can be updated each iteration as the following.

$$\{F_{ext\ i}^{j}\} = \{F_{ext\ i-1}^{j}\} + \Delta\lambda_i^j\ \{\Delta F_{ext}^{\wedge}\} \quad (45)$$

where, $\{\Delta F_{ext}^{\wedge}\}$ is the reference load vector, including updating fixed end forces. The factor $\Delta\lambda_j^i$ is the load increment factor for the jth iteration in the ith increment, which is calculated according to the adopted nonlinear solution strategy depending on the vectors from previous iteration.

5 NUMERICAL EXAMPLES

This section contains various numerical verifications to check the accuracy and ability of the present work. There were no many available numerical examples for plastic analysis of steel frames loaded along the elements' span. The available benchmark frames were solved using the proposed model. Also, additional novel examples were prepared for different types of loading.

5.1 Vogel's Multi Story Plan Frame

The well-known six story frame, in Figure 12, presented by Vogel [55] and solved using plastic zone methodology. The steel modulus of elasticity was assumed as 205 GPa, and the yield stress as 235 MPa. The columns of frame are exposed to out of plumpness as initial imperfection, with an inclination 1/450 for the six stories.

Many researchers used this example as a calibrating frame for their own models such as the work in [56] and [57], also the work in [58] resolved the frame but neglecting the residual stresses. Usually, the researchers divide the beams into more than one element to models span uniform loads as nodal loads, such as [56], [57], and [49]. The present research solves this dilemma as the proposed element allows span loads without dividing the member also the plasticity spread can be captured and represented. The frame was solved in the current work, including and excluding residual stress effects, using only ingle beam-column element for each member. The results are presented in Figure 13 and Figure 14 show the

accuracy of the presented model in tracing geometric and material nonlinear manner.

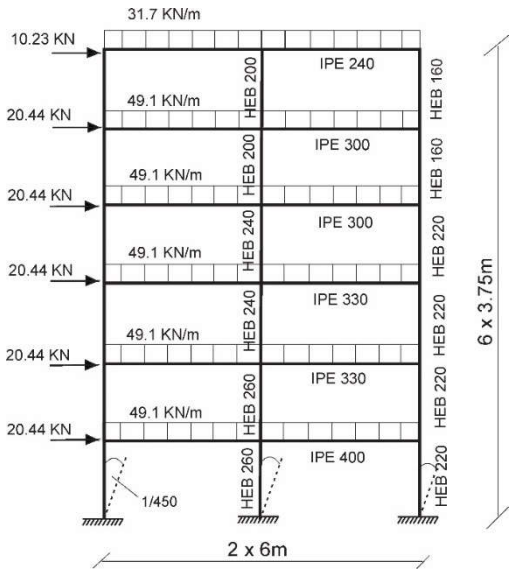

Figure 12: Vogel's Six Story Frame

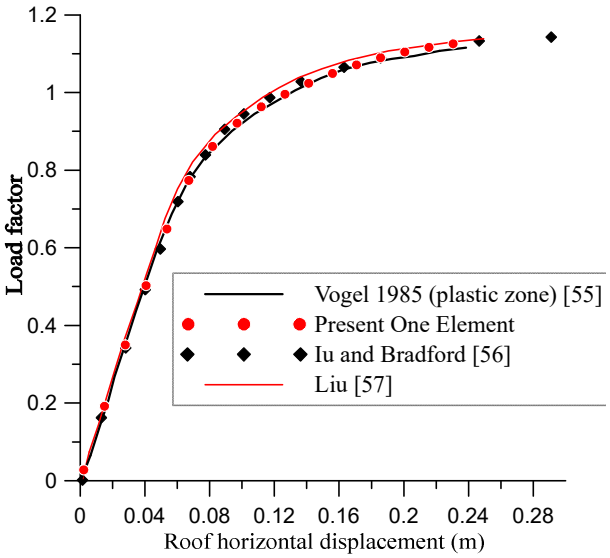

Figure 13: Load Displacement Curve for Vogel's Frame Considering Residual Stresses

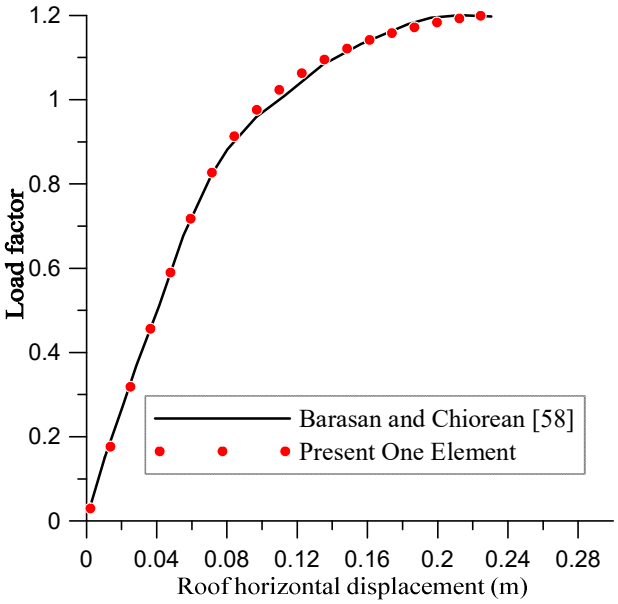

Figure 14: Load Displacement Curve for Vogel's Frame without Residual Stresses

5.2 Two Bay Four Story Plan Frame

The two bay four story frame shown in Figure 15 was analyzed in many researches as a benchmark frame for inelastic analysis. The steel material of the frame has 200 GPa and 250 MPa for elastic modulus and yield stress, respectively. The frame was solved by Doan-Ngoc *et al.* [59] and by Kukreti and Zhou [60]. In the present work, the frame was modeled using only one element for each member, unlike the work in [59] which divided the beams into two elements. The analysis results, shown in Figure 16, illustrate the accuracy of the deduced model in tracing geometric and material nonlinearities.

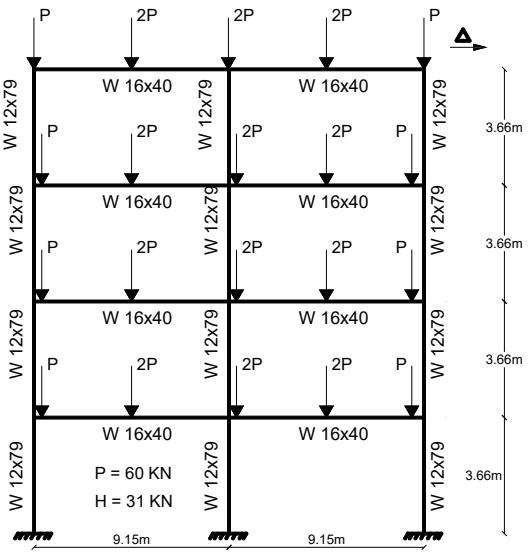

Figure 15: Geometry of Two Bay Four Story Frame

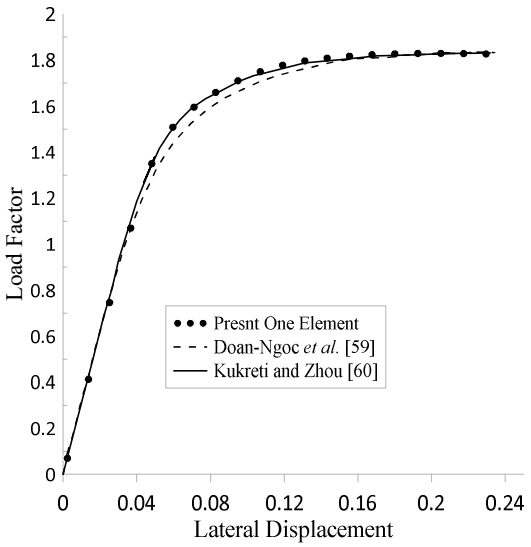

Figure 16: Load Displacement Curve for Two Bay Four Story Frame

5.3 Two Story Space Frame Under Span Loads

Coung and Kim [61] presented a solved example for two story space frame loaded with concentrated forces at nodes only. They have used a fine mesh of shell elements to get a reference solution via ABAQUS software. The present work is related to frames with lateral span loads, so the geometry of the example from [61] has been employed but the loads are different. Figure 17 show the geometry of the space frame which has a cross section H 150x160x10x6.5, with steel material properties 221 GPa and 320 MPa for the elastic modulus and yield stress, respectively. The frame has been modelled in the present work using a fine mesh of shell elements including the same geometric initial out straightness detailed in [61] and the initial residual stresses from ECCS [62]. The performed ABAQUS model, in Figure 19, prevented effects of joint local deformation by using stiffeners with higher grade steel material. To calibrate our mode, the frame was solved firstly under the same nodal loads from [61] and the results were identical.

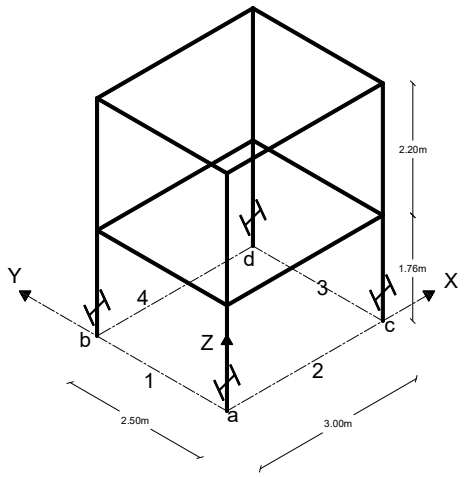

Figure 17: Two Story Space frame with H-Shaped Section

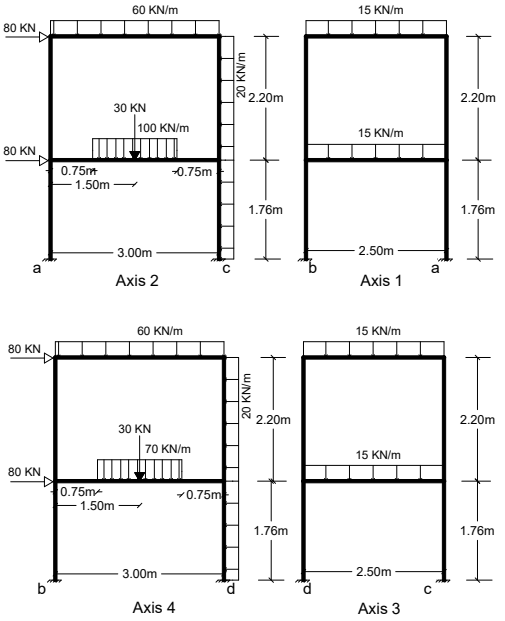

Figure 18: Loads on Two Story Space frame with H-Shaped Section

The frame has been solved using the prepared ABAQUS model in the present research under the loading condition shown in Figure 18, which includes various of loading shapes. The distribution of stresses along the frame member is shown in Figure 21, which illustrates the plasticity spread at many positions along the span rather than members' ends. After that, the frame has been solved using the proposed model in the current research based on beam-column element. Only one element per each member was used in the analysis. Figure 20 shows the resulting problem size un ABAQUS, which is compared to the proposed model of twelve nodes only. The proposed beam-column model has the ability to model and trace distributed plasticity, and also allows for lateral loads along the member span. For the members with two different loads, the principles of super position were employed by tacking the contribution of each load and summing them either in first or second order parameters and also in calculating the bowing terms. Neglecting the interaction between the forces on the second order parameters of each other's seems to have no significant effect on the analysis results, which can be attributed to the small strain assumption.

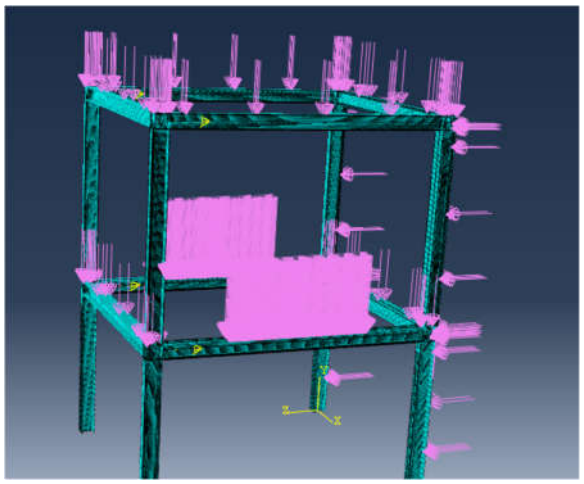

(a)

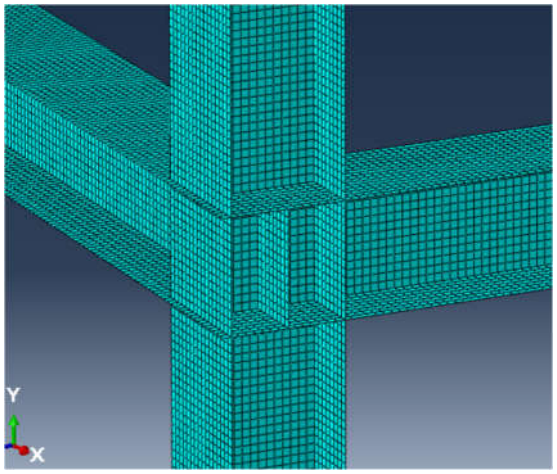

(b)

Figure 19: Modelling of Two-Story Space Frame by ABAQUS; a) General View of Frame, b) Stiffeners at Frame Joints

The load displacement curve is compared from the solution by ABAQUS model and the proposed beam-column model in Figure 22 which assure the accuracy of the proposed model in tracing geometric and material nonlinearities even with distributed plasticity and member span loads.

```
                    P R O B L E M   S I Z E

NUMBER OF ELEMENTS IS                                    175661
NUMBER OF ELEMENTS DEFINED BY THE USER AND *TIE          175648
NUMBER OF INTERNAL ELEMENTS GENERATED FOR CONTACT             1
NUMBER OF NODES IS                                       178802
NUMBER OF NODES DEFINED BY THE USER                      178800
NUMBER OF INTERNAL NODES GENERATED BY THE PROGRAM             2
TOTAL NUMBER OF VARIABLES IN THE MODEL                 1072803
(DEGREES OF FREEDOM PLUS MAX NO. OF ANY LAGRANGE MULTIPLIER
 VARIABLES. INCLUDE *PRINT,SOLVE=YES TO GET THE ACTUAL NUMBER.)
```

Figure 20: Data from ABAQUS model

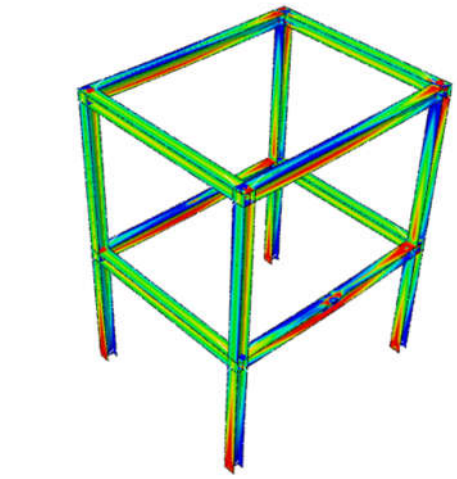

Figure 21: Stress Distribution at Frame Members

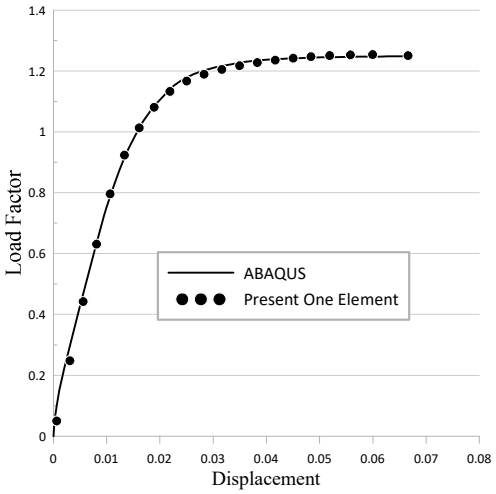

(a)

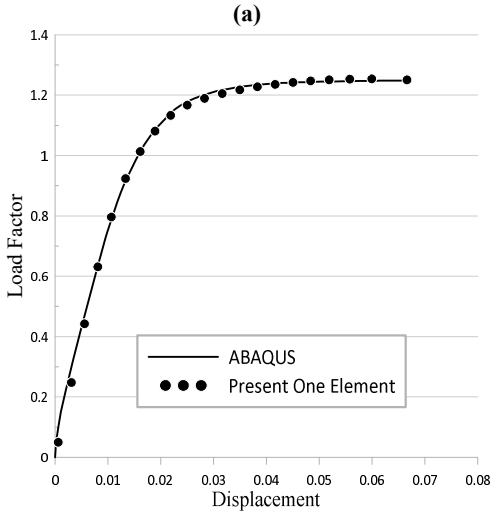

(b)

Figure 22: Load Displacement Curve for Two-Story Space Frame; a) Displacement at First Floor, b) Displacement at Roof

5.4 Cantilever Columns

To check the proposed model for different loading shapes, a cantilever example was prepared using ABAQUS software. A fine mesh of shell elements was used in modelling to represent inelasticity and second order effects accurately.

5.4.1. Cantilever with Uniform Distributed Lateral Load

The cantilever member in Figure 23 has a cross section of H 257 x 254 x 9.4 x 15.6 with a steel material having properties of 400 MPa and 200 GPa for yield stress and Yong's Modulus, respectively. The initial residual stresses were considered according to the proposed by (ECCS)[62]. Two different cases of loading were considered to check the model under different contribution of geometric and material nonlinearities, and the column is bent about its major axis. The load displacement curve, in Figure 24, shows the analysis results of the proposed one element per member model and the fine mesh model by ABAQUS.

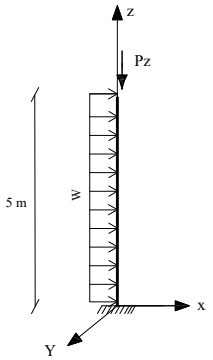

Figure 23: Cantilever under Lateral Uniform Load

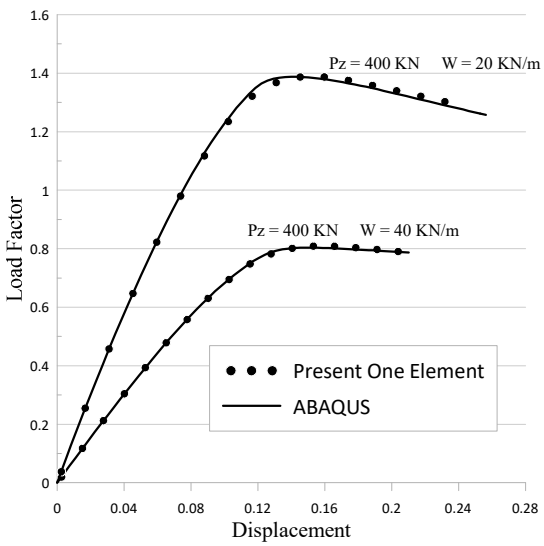

Figure 24: Load-Displacement Curve for Cantilever under Lateral Uniform Load

5.4.2. Cantilever with Triangular Lateral Load

The cantilever member in Figure 25 has the same cross section and steel material of the column in Section 5.4.1. However, the column is subjected to triangular span load in addition to loads at tip point.

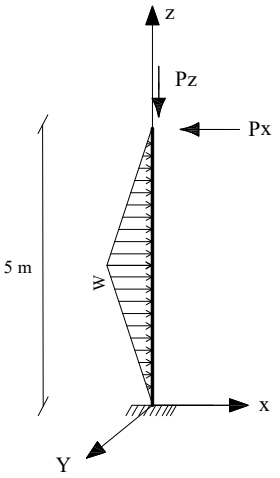

Figure 25: Cantilever under Lateral Triangular Load

The initial residual stresses by (ECCS)[62]were considered, and the analysis is performed using both of the proposed beam column element and ABAQUS shell elements. The comparison between the results is declared in Figure 26, which illustrates the ability of the proposed model to trace plasticity spread and second order effects.

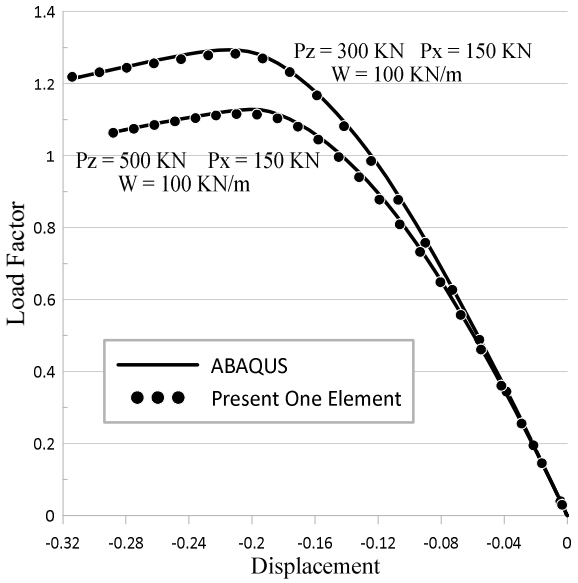

Figure 26: Load-Displacement Curve for Cantilever under Lateral Uniform Load

Figure 27 shows both unloaded and loaded state of the column. The unloaded state includes initial residual stresses only, but after loading process the plasticity spread can be noted along the span of the member and that cannot be captured using the plastic hinge approach.

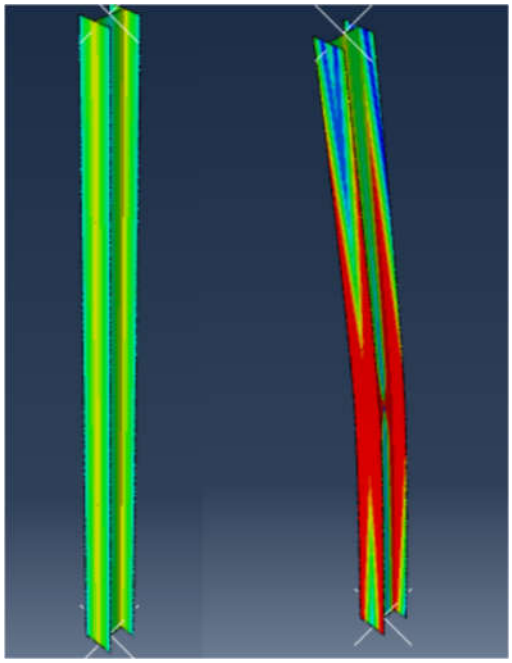

Figure 27: Stress Distribution at Cantilever Column Before and After Loading

6 CONCLUSION

This work presented a novel beam-column element for distributed plasticity inelastic analysis of steel frames. The proposed model was based on the one element per member approach and modeled geometric and material nonlinear effects. The change of element stiffness matrix due to the plasticity spread along the member and the geometric nonlinearity has been modeled, and the used analysis procedure allowed to trace these effects throughout the analysis steps. A major contribution of this work is allowing span transverse loads to be included in the analysis without dividing the frame member to many elements. New formulas for calculating fixed end moments due to numerous shapes of span loads have been presented. These formulas take into consideration the redistribution of fixed end moments due to the distributed plasticity. For second order parameters related to span loads, new formulas for different shapes of loads have been found based on the fifth order displacement function in addition to those previously presented in [50].

An appropriate analysis procedure has been prepared and was employed in a finite element program based on the proposed model. Numerous examples have been solved using the proposed model. In addition to the available benchmarked frames, novel solved examples have been prepared and solved to check the reliability of the model in case of different shapes of loads. The proposed model showed sufficient accuracy in modeling steel frames in nonlinear analysis. The one element per member approach helped in saving time of the analysis without compromising the accuracy of solutions.

7 APPENDECIES

A. 1- List of symbols

v Displacement of the element
M_z Bending moment about Z axis
M_y Bending moment about Y axis
P Axial force
θ_z Flexural rotation around Z axis
θ_y Flexural rotation around Y axis
ξ Distance parameter ratio
EA Axial rigidity
q Axial force parameter
C_{ii} Term of minor bending stiffness
C_{ij} Term of major bending stiffness
b_1 bowing function 1
b_2 bowing function 2
b_m bowing function due to span load 1
b_s bowing function due to span load 2
σ_y Yield stress
I_z Bending rigidity about Z axis for the member
EI_y Bending rigidity about Y axis for the member
EI_{zk} Internal segment's rigidity about Z axis
EI_{zy} Internal segment's rigidity about Y axis
C_{mz} First-Order stiffness about Z axis
C_{my} First-Order stiffness about Y axis
C_{gz} Second-Order bending stiffness about Z axis
C_{gy} Second-Order bending stiffness about Y axis
$G_{1\alpha}$ Coupling term
$G_{2\alpha}$ Coupling term
H_α Coupling term
GJ Torsional rigidity
η Torsional stiffness
$[K_T]$ Tangent stiffness matrix
$[T]$ Transformation matrix to 12x12

A. 2- Matrices formulation

$$[\mathrm{T}] = \begin{pmatrix} 0 & \frac{1}{L} & 0 & 0 & 0 & 1 & 0 & -\frac{1}{\mathrm{L}} & 0 & 0 & 0 & 0 \\ 0 & \frac{1}{\mathrm{L}} & 0 & 0 & 0 & 0 & 0 & -\frac{1}{\mathrm{L}} & 0 & 0 & 0 & 1 \\ 0 & 0 & -\frac{1}{\mathrm{L}} & 0 & 1 & 0 & 0 & 0 & \frac{1}{\mathrm{L}} & 0 & 0 & 0 \\ 0 & 0 & -\frac{1}{\mathrm{L}} & 0 & 0 & 0 & 0 & 0 & \frac{1}{\mathrm{L}} & 0 & 1 & 0 \\ 0 & 0 & 0 & -1 & 0 & 0 & 0 & 0 & 0 & 1 & 0 & 0 \\ -1 & 0 & 0 & 0 & 0 & 0 & 1 & 0 & 0 & 0 & 0 & 0 \end{pmatrix} \quad (A.1)$$

T is the matrix transforms [6x6] stiffness matrix to [12x12] including shear stiffness in corotational coordinating approach.

$$K_T = \begin{pmatrix} c_{zii} + \frac{EI_{eq_z}}{L}\frac{G_{1z}^2}{H_z} & c_{zij} + \frac{EI_{eq_z}}{L}\frac{G_{1z}G_{2z}}{H_z} & \frac{EI_{eq_z}}{L}\frac{G_{1z}G_{1y}}{H_z} & \frac{EI_{eq_z}}{L}\frac{G_{1z}G_{2y}}{H_z} & 0 & \frac{EI_{eq_z}}{L}\frac{G_{1z}}{LH_z} \\ & c_{zjj} + \frac{EI_{eq_z}}{L}\frac{G_{1z}^2}{H_z} & \frac{EI_{eq_z}}{L}\frac{G_{2z}G_{1y}}{H_z} & \frac{EI_{eq_z}}{L}\frac{G_{2z}G_{2y}}{H_z} & 0 & \frac{EI_{eq_z}}{L}\frac{G_{2z}}{LH_z} \\ & & c_{yii} + \frac{EI_{eq_y}}{L}\frac{G_{1y}^2}{H_y} & c_{yij} + \frac{EI_{eq_y}}{L}\frac{G_{1y}G_{2y}}{H_y} & 0 & \frac{EI_{eq_y}}{L}\frac{G_{1y}}{LH_y} \\ & & & c_{yjj} + \frac{EI_{eq_y}}{L}\frac{G_{1y}^2}{H_y} & 0 & \frac{EI_{eq_y}}{L}\frac{G_{2y}}{LH_y} \\ & & symmetrical & & T & 0 \\ & & & & & \frac{EI}{L^3H} \end{pmatrix}$$

$[K_T]$ tangent stiffness matrix in corotational formulation.

8 REFERENCES

[1] “Specification for Structural Steel Buildings Supersedes the Specification for Structural Steel Buildings,” 2022.

[2] Yang, Y. B., Anquan Chen, and Song He. "Research on nonlinear, postbuckling and elasto-plastic analyses of framed structures and curved beams." Meccanica 56 (2021): 1587-1612.

[3] Zhang ZJ, Chen BS, Bai R, Liu YP. Non-linear behavior and design of steel structures: Review and outlook. Buildings. 2023 Aug 21;13(8):2111.

[4] Oran C. Tangent stiffness in space frames. Journal of the Structural Division. 1973 Jun;99(6):987-1001.

[5] Kassimali A, Abbasnia R. Large deformation analysis of elastic space frames. Journal of structural Engineering. 1991 Jul;117(7):2069-87.

[6] Teh LH, Hsiao KM, White DW, Ziemian RD, Chan SL, Gu JX. Exact tangent stiffness for imperfect beam-column members. Journal of Structural Engineering. 2001 Dec;127(12):1490-2.

[7] Kim SE, Uang CM, Choi SH, An KY. Practical advanced analysis of steel frames considering lateral-torsional buckling. Thin-walled structures. 2006 Jul 1;44(7):709-20.

[8] Meek JL, Tan HS. Geometrically nonlinear analysis of space frames by an incremental iterative technique. Computer methods in applied mechanics and engineering. 1984 Dec 1;47(3):261-82.
[9] Chajes A, Churchill JE. Nonlinear frame analysis by finite element methods. Journal of structural engineering. 1987 Jun;113(6):1221-35.
[10] Teh LH. Cubic beam elements in practical analysis and design of steel frames. Engineering structures. 2001 Oct 1;23(10):1243-55.
[11] Chan SL, Zhou ZH. Pointwise equilibrating polynomial element for nonlinear analysis of frames. Journal of structural engineering. 1994 Jun;120(6):1703-17.
[12] Chan SL, Zhou ZH. Second-order elastic analysis of frames using single imperfect element per member. Journal of Structural Engineering. 1995 Jun;121(6):939-45.
[13] Liu SW, Liu YP, Chan SL. Pushover analysis by one element per member for performance-based seismic design. International Journal of Structural Stability and Dynamics. 2010 Mar;10(01):111-26.
[14] Iu J. Analysis of steel structures for first-and second-order element (displacement and force) solutions. InProceedings of the 10th Pacific Structural Steel Conference (PSSC 2013) 2013 (pp. 1-6). Research Publishing Services.
[15] Tang YQ, Liu YP, Chan SL, Du EF. An innovative co-rotational pointwise equilibrating polynomial element based on Timoshenko beam theory for second-order analysis. Thin-Walled Structures. 2019 Aug 1;141:15-27.
[16] Iu CK, Bradford MA. Second-order elastic finite element analysis of steel structures using a single element per member. Engineering Structures. 2010 Sep 1;32(9):2606-16.
[17] Truong VH, Nguyen PC, Kim SE. An efficient method for optimizing space steel frames with semi-rigid joints using practical advanced analysis and the micro-genetic algorithm. Journal of Constructional steel research. 2017 Jan 1;128:416-27.
[18] Kassimali A. Large deformation analysis of elastic-plastic frames. Journal of structural engineering. 1983 Aug;109(8):1869-86.
[19] Tang YQ, Zhu H, Liu YP, Ding YY, Chan SL. A novel efficient plastic hinge approach for direct analysis of steel structures. Engineering Structures. 2024 Nov 15;319:118837.
[20] Chen WF, Chan SL. Second-order inelastic analysis of steel frames using element with midspan and end springs. Journal of Structural Engineering. 1995 Mar;121(3):530-41.
[21] Shugyo M. Elastoplastic large deflection analysis of three-dimensional steel frames. Journal of Structural Engineering. 2003 Sep;129(9):1259-67.
[22] Wei L, Ganping S, Siulai C. Research on Advanced Analysis Method of Semi-Rigid Steel Frames. The Open Construction & Building Technology Journal. 2015 May 29;9(1).
[23] Ngo-Huu C, Nguyen PC, Kim SE. Second-order plastic-hinge analysis of space semi-rigid steel frames. Thin-Walled Structures. 2012 Nov 1;60:98-104.
[24] Chan SL, Chui PP. A generalized design-based elastoplastic analysis of steel frames by section assemblage concept. Engineering Structures. 1997 Aug 1;19(8):628-36.
[25] Dang HK, Thai DK, Kim SE. Stochastic analysis of semi-rigid steel frames using a refined plastic-hinge model and Latin hypercube sampling. Engineering Structures. 2023 Sep 15;291:116313.
[26] Liew JY, Chen WF. Implications of using refined plastic hinge analysis for load and resistance factor design. Thin-walled structures. 1994 Jan 1;20(1-4):17-47.
[27] Iu CK. Nonlinear analysis for the pre-and post-yield behavior of a composite structure with the refined plastic hinge approach. Journal of Constructional Steel Research. 2016 Mar 1;119:1-6.
[28] Nguyễn VT, Phạm TB, Nguyễn XB. Refined second-order plastic-hinge dynamic analysis for planar steel frames. InJournal of Physics: Conference Series 2019 Dec 1 (Vol. 1425, No. 1, p. 012047). IOP Publishing.
[29] Zhou Y, Hu B, Gong Y, Tang L, Li Y. Second-order improved refined plastic hinge method with implementation of continuous strength method. Journal of Constructional Steel Research. 2023 Dec 1;211:108169.
[30] Zhou Y, Ning S, Huang D, Li Y. Refined plastic hinge method for steel frames with local–global interactive buckling. Thin-Walled Structures. 2022 Dec 1;181:110013.
[31] Lee S, Kim T, Lieu QX, Vo TP, Lee J. A novel data-driven analysis for sequentially formulated plastic hinges of steel frames. Computers & Structures. 2023 Jun 1;281:107031.
[32] Kim SE, Kim Y, Choi SH. Nonlinear analysis of 3-D steel frames. Thin-walled structures. 2001 Jun 1;39(6):445-61.
[33] Wang Y, Wang Q, Dong J, Peng Y. Ultimate analysis of steel structures based on fiber hinge model and time-varying structure theory. International Journal of Steel Structures. 2015 Sep;15:567-79.
[34] Cuong NH, Seung-Eock KI. Practical nonlinear analysis of steel–concrete composite frames using fiber–hinge method. Journal of

Constructional Steel Research. 2012 Jul 1;74:90-7.
[35] Nguyen PC, Kim SE. A new improved fiber plastic hinge method accounting for lateral-torsional buckling of 3D steel frames. Thin-Walled Structures. 2018 Jun 1;127:666-75.
[36] Zhou Y, Huang D, Li T, Li Y. Second-order arbitrarily-located-refined plastic hinge model for high-strength steel frame design. Journal of Constructional Steel Research. 2022 Mar 1;190:107112.
[37] El-Zanaty M, Murrary D, Bjorhovde R. Inelastic behavior of multistory steel frames. In: Structural engineering report Mo. 83. Alberta, Canada, University of Alberta; 1980.
[38] Chiorean CG, Barsan GM. Large deflection distributed plasticity analysis of 3D steel frameworks. Computers & structures. 2005 Jul 1;83(19-20):1555-71.
[39] Chiorean CG, Marchis IV. A second-order flexibility-based model for steel frames of tapered members. Journal of Constructional Steel Research. 2017 May 1;132:43-71.
[40] Le-Van B, Chiorean CG, Kim SE, Ngo-Huu C. Nonlinear inelastic analysis of space semi-rigid steel frames subjected to static load using plastic-zone method. Mechanics of Advanced Materials and Structures. 2024 Dec 2;31(27):9497-516.
[41] Du ZL, Ding ZX, Liu YP, Chan SL. Advanced flexibility-based beam-column element allowing for shear deformation and initial imperfection for direct analysis. Engineering Structures. 2019 Nov 15;199:109586.
[42] Chen WF, Liu YP, Du ZL, Bai R, Chan SL. A consistent tapered beam-column element allowing for different variations and initial imperfections. InStructures 2021 Oct 1 (Vol. 33, pp. 3443-3460). Elsevier.
[43] Viana HF, da Silva RG, Costa RS, Lavall AC. Formulation for nonlinear dynamic analysis of steel frames considering the plastic zone method. Engineering Structures. 2020 Nov 15;223:111197.
[44] Zubydan AH. A simplified model for inelastic second order analysis of planar frames. Engineering Structures. 2010 Oct 1;32(10):3258-68.
[45] Zubydan AH. Inelastic large deflection analysis of space steel frames including H-shaped cross sectional members. Engineering Structures. 2013 Mar 1;48:155-65.
[46] Zubydan AH. Inelastic second order analysis of steel frame elements flexed about minor axis. Engineering Structures. 2011 Apr 1;33(4):1240-50.
[47] Sharaf T, Hanefa A, Zubydan A, Elghandour M, Elsabbagh A. Axial Force and Biaxial Bending Interaction for I-Shaped Cross Section. Practice Periodical on Structural Design and Construction. 2021 Nov 1;26(4):04021042. 2021, doi: 10.1061/(asce)sc.1943-5576.0000609.
[48] ElSabbagh A, Hanefa A, Zubydan A, ElGhandour M, Sharaf T. Inelastic large deflection analysis of space steel frames consisting of I-shaped cross section. Steel and Composite Structures, An International Journal. 2021 Dec;41(6):887-98.
[49] Zubydan AH, ElSabbagh AI, Sharaf T, Farag AE. Inelastic large deflection analysis of space steel frames using an equivalent accumulated element. Engineering Structures. 2018 May 1;162:121-34.
[50] Zhou ZH, Chan SL. Refined second-order analysis of frames with members under lateral and axial loads. Journal of Structural Engineering. 1996 May;122(5):548-54.
[51] Kim SE, Choi SH. Practical second-order inelastic analysis for three-dimensional steel frames subjected to distributed load. Thin-walled structures. 2005 Jan 1;43(1):135-60.
[52] Iu J, Bradford M. Novel non-linear elastic structural analysis with generalised transverse element loads using a refined finite element. Advanced Steel Construction. 2015;11(2):223-49.
[53] Iu CK. Generalised element load method for first-and second-order element solutions with element load effect. Engineering Structures. 2015 Jun 1;92:101-11.
[54] Iu CK. Generalised element load method with whole domain accuracy for reliable structural design. Advanced Steel Construction. 2016 Dec 1;12(4):466-86.
[55] Vogel, U., 1985. Calibrating frames. Stahlbau, 10(10), pp.1-7.
[56] Iu CK, Bradford M. Higher-order non-linear analysis of steel structures. Part II: refined plastic hinge formulation. Advanced Steel Construction. 2012;8(2):183-98.
[57] Liu, Siwei. "Second-order design and advanced analysis of hybrid steel and concrete framed structures." PhD, The Hong Kong Polytechnic University, Hong Kong, 2013.
[58] Barsan GM, Chiorean CG. Influence of residual stress on the carrying capacity of steel framed structures. numerical investigation. Stability and Ductility Steel Structures, SDSS. 1999 Aug 3;99:317-24.
[59] Doan-Ngoc TN, Dang XL, Chu QT, Balling RJ, Ngo-Huu C. Second-order plastic-hinge analysis of planar steel frames using corotational beam-column element. Journal of Constructional Steel Research. 2016 Jun 1;121:413-26.

[60] Kukreti AR, Zhou FF. Eight-bolt endplate connection and its influence on frame behavior. Engineering structures. 2006 Sep 1;28(11):1483-93.
[61] Ngo-Huu C, Kim SE. Practical advanced analysis of space steel frames using fiber hinge method. Thin-Walled Structures. 2009 Apr 1;47(4):421-30.
[62] European Convention for Constructional Steelwork. Advisory Committee 5, Application of Eurocode 3. Essentials of Eurocode 3: Design Manual for Steel Structures in Building. ECCS.